

# Suppression of Superconductivity by Néel-Type Magnetic Fluctuations in the Iron Pnictides

Rafael M. Fernandes<sup>1,2,\*</sup> and Andrew J. Millis<sup>1</sup>

<sup>1</sup>*Department of Physics, Columbia University, New York, New York 10027, USA*

<sup>2</sup>*Theoretical Division, Los Alamos National Laboratory, Los Alamos, New Mexico 87545, USA*

(Received 16 August 2012; revised manuscript received 8 November 2012; published 14 March 2013)

Motivated by the recent experimental detection of Néel-type  $[(\pi, \pi)]$  magnetic fluctuations in some iron pnictides, we study the impact of competing  $(\pi, \pi)$  and  $(\pi, 0)$  spin fluctuations on the superconductivity of these materials. We show that, counterintuitively, even short-range, weak Néel fluctuations strongly suppress the  $s^{+-}$  state, with the main effect arising from a repulsive contribution to the  $s^{+-}$  pairing interaction, complemented by low-frequency inelastic scattering. Further increasing the strength of the Néel fluctuations leads to a low- $T_c$   $d$ -wave state, with a possible intermediate  $s + id$  phase. The results suggest that the absence of superconductivity in a series of hole-doped pnictides is due to the combination of short-range Néel fluctuations and pair-breaking impurity scattering and also that  $T_c$  of optimally doped pnictides could be further increased if residual  $(\pi, \pi)$  fluctuations were reduced.

DOI: [10.1103/PhysRevLett.110.117004](https://doi.org/10.1103/PhysRevLett.110.117004)

PACS numbers: 74.70.Xa, 74.20.Mn, 74.20.Rp, 74.25.Bt

The proximity of the superconducting (SC) state to a “stripe” spin-density wave (SDW) instability in the phase diagrams of the recently discovered iron-based superconductors (FeSC) [1] prompted the proposal that SDW spin fluctuations provide the pairing mechanism [2]. Indeed, the Fermi surface (FS) of many iron pnictides consists of electron pockets displaced from central hole pockets by the SDW ordering vector  $\mathbf{Q}_{\text{SDW}} = (\pi, 0)/(0, \pi)$  (see Fig. 1). In this situation, even weak SDW fluctuations may overcome a strong on-site repulsion giving rise to an  $s^{+-}$  SC state, in which the gap function has one sign on the electron pockets and another sign on the hole pockets [3].

However, the two electron pockets in Fig. 1 are connected by the momentum  $\mathbf{Q}_{\text{Néel}} = (\pi, \pi)$ , suggesting that Néel-type magnetic fluctuations may also be important [4]. These fluctuations favor a  $d$ -wave SC state in which the gap function has an opposite sign in the two electron pockets. On the theory side, first-principle and Hartree-Fock calculations find that the Néel state is locally stable but with a higher energy than the SDW state [5,6], whereas random phase approximation calculations performed in the paramagnetic phase find a peak in the magnetic susceptibility at  $\mathbf{Q}_{\text{Néel}}$ , which is, however, weaker than the peak at  $\mathbf{Q}_{\text{SDW}}$  [7].

Experimentally, neutron scattering measurements [8] revealed that even at small  $x$  values,  $\text{Ba}(\text{Fe}_{1-x}\text{Mn}_x)_2\text{As}_2$  exhibits spin fluctuations peaked at  $\mathbf{Q}_{\text{Néel}}$ , in addition to the SDW fluctuations peaked at  $\mathbf{Q}_{\text{SDW}}$ . NMR measurements [9] confirmed that these Néel fluctuations couple to the conduction electrons. Because the entire family of “in-plane” hole-doped  $\text{Ba}(\text{Fe}_{1-x}\text{M}_x)_2\text{As}_2$  compounds ( $M = \text{Mn}, \text{Cr}, \text{Mo}$ ) [10] displays SDW order at  $x = 0$  and Néel order at  $x = 1$ , we expect that competing Néel and SDW fluctuations will be found across the whole material family. Intriguingly, superconductivity has not been reported in these materials to date [11], in contrast

to the electron-doped counterparts  $M = \text{Co}, \text{Ni}, \text{Rh}, \text{Pt}, \text{Cu}$ , where SC is always observed [12].

There is also indirect evidence for Néel fluctuations in the extremely electron-doped  $A_y\text{Fe}_{2-x}\text{Se}_2$  compounds [13]. In these materials, the near absence of FS pockets in the center of the Brillouin zone suggests that SDW fluctuations and the  $s^{+-}$  state are disfavored, whereas the squarelike shape of the electron pockets is expected to enhance the  $(\pi, \pi)$  fluctuations [14]. Chemical substitution on the  $A$  site or application of pressure [15] can create a small pocket in the center of the Brillouin zone, which could support  $(\pi, 0)$  fluctuations and  $s^{+-}$  SC.

The effect of competing spin fluctuations on FeSCs is thus of experimental and theoretical interest. In this Letter, we address the problem via a multiband Eliashberg approach [16,17] in which the effect of spin fluctuations on electrons is determined from the one-loop self-energy (see Fig. 1). This approximation has been extensively employed in studies of cuprates [18–20], ferromagnetic SC [21], and pnictides [22]. Our calculation goes beyond

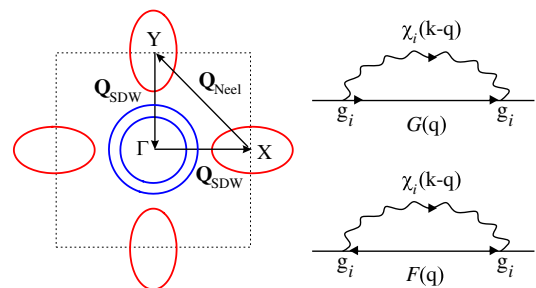


FIG. 1 (color online). (left panel) Schematic Fermi surface configuration in the 1-Fe Brillouin zone, with two central hole pockets and two electron pockets. (right panel) Self-energy diagrams of the Eliashberg equations: normal component (upper panel) and anomalous component (lower panel).

previous work [22] by incorporating both SDW and Néel fluctuations, including the Coulomb pseudopotential, and using the experimentally determined spin fluctuation spectrum instead of the single-pole approximation employed previously.

We find that the Coulomb pseudopotential has only a weak effect on the dominant  $s^{+-}$  state but even weak short-range Néel fluctuations strongly suppress the transition temperature  $T_c^{s\text{-wave}}$ . If sufficiently strong, the Néel fluctuations may induce a  $d$ -wave state, but the transition temperature is found to be much lower than the optimal  $T_c$  for the  $s^{+-}$  state. The transition between  $s^{+-}$  and  $d$ -SC may either occur via an intermediate time reversal symmetry-breaking  $s + id$  state [23,24] or, if the impurity scattering is stronger, via an intermediate non-SC state separating the two regions (see Fig. 2).

To gain insight into the results, we use the functional derivative methods of Bergmann and Rainer [25,26]. We find that the strong suppression of the  $s^{+-}$  state comes mostly from a repulsive  $s^{+-}$  pairing interaction induced by the Néel fluctuations, although pair-breaking inelastic scattering plays some role. Finally, we discuss the implications of our results not only to the SC of the in-plane hole-doped pnictides but also to the value of  $T_c$  in the FeSCs in general.

Our model consists of a two-dimensional FS with two central hole pockets ( $\Gamma$ , density of states  $N_\Gamma$ ) and two electron pockets ( $X$  and  $Y$ , density of states  $N_X$ ) displaced from the center by the momenta  $(\pi, 0)$  and  $(0, \pi)$  (Fig. 1)

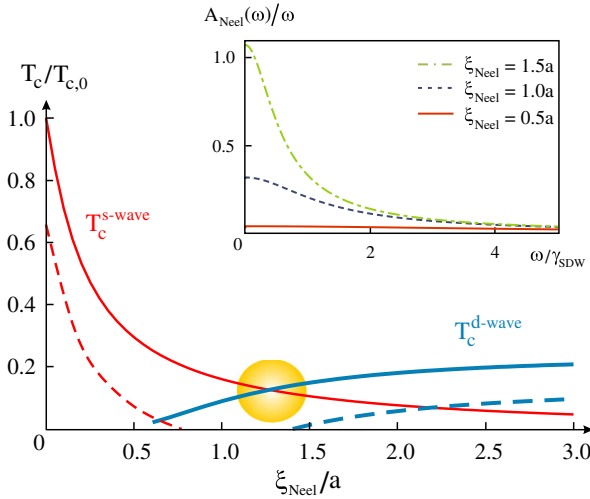


FIG. 2 (color online). Transition temperatures  $T_c$  of the  $s$ -wave (red, lighter line curve) and  $d$ -wave (blue, heavier line curve) states as a function of the Néel magnetic correlation length  $\xi_{\text{Néel}}$ , for  $r = 0.65$ ,  $\gamma_{\text{Néel}}/\gamma_{\text{SDW}} = 0.33$ ,  $\lambda_{\text{Néel}}/\lambda_{\text{SDW}} = 2$ , and  $\mu^* = 0.8$ .  $T_{c,0} \approx 0.1\gamma_{\text{SDW}}$  is the  $s^{+-}$  transition temperature for  $\xi_{\text{Néel}} = 0$ . The shaded area denotes the regime where the two states have similar transition temperatures and a possible  $s + id$  state may occur. The dashed lines show the behavior of the system in the presence of impurity scattering, with  $\tau^{-1} \approx 0.1T_{c,0}$ . The inset shows the frequency dependence of the spectral function  $A_{\text{Néel}}(\omega)$  of the Néel fluctuations for different values of  $\xi_{\text{Néel}}$ .

[27]. For simplicity, hereafter we assume that these two hole pockets are degenerate—our results do not depend on this simplification. Following Ref. [28], we set  $r = N_X/N_\Gamma = 0.65$ . The electrons are coupled to two types of low-energy bosonic excitations, namely, SDW spin fluctuations peaked at  $(\pi, 0)/(0, \pi)$  and Néel spin fluctuations peaked at  $(\pi, \pi)$ . Experiment (Refs. [8,29]) indicates that in the paramagnetic phase these excitations are described by diffusive dynamic susceptibilities

$$\chi_i^{-1}(\mathbf{Q}_i + \mathbf{q}, \Omega_n) = \xi_i^{-2} + q^2 + \gamma_i^{-1}|\Omega_n|. \quad (1)$$

Here,  $\mathbf{q}$  is the momentum deviation from the ordering vector  $\mathbf{Q}_i$  (all lengths are in units of the lattice parameter  $a$ ) and  $\Omega_n$  is the bosonic Matsubara frequency. The quantity that actually enters the Eliashberg equations is the spectral function integrated over the momentum component  $q_{\parallel}$  parallel to the FS and evaluated at  $q_{\perp} = 0$ , i.e.,  $A_{\text{Néel}}(\omega) = \int dq_{\parallel} \text{Im} \chi_{\text{Néel}}(q_{\parallel}, \omega)$ . This spectral function gives rise to the Matsubara-axis interaction  $a^{(i)}(\Omega_n) = \xi_i/\sqrt{1 + |\Omega_n|\gamma_i^{-1}\xi_i^2}$ , which enters the Eliashberg equations as described below. Note that the orbital character of the low energy states varies with position around the FS. In the Eliashberg formalism, the resulting angular dependence of the interaction parameters is averaged over the FS, so as shown in the Supplemental Material [30] the variation in the orbital character only affects the values of the effective coupling constants.

The spin fluctuations in each momentum channel  $i$  are described by two parameters: the Landau damping  $\gamma_i$ , which sets the energy scale, and the correlation length  $\xi_i$ , which sets both the strength and the spatiotemporal correlations of the spin fluctuations. We will tune the spectrum by varying  $\xi_i$ . Because the Landau damping originates from the low-energy decay of the spin excitations into electron-hole pairs,  $\gamma_i$  is determined by the electron-boson coupling constant  $g_i$  and the densities of states. The coupling  $g_{\text{SDW}}$  is set to yield  $T_{c,0}^{s\text{-wave}} \approx 30$  K. Following the experimental results of Ref. [8], we use  $\gamma_{\text{Néel}}/\gamma_{\text{SDW}} \approx 0.33$  with  $\gamma_{\text{SDW}} \approx 25$  meV; the value of  $g_{\text{Néel}}$  follows from the relationship between  $\gamma_{\text{Néel}}/\gamma_{\text{SDW}}$  and  $g_{\text{Néel}}/g_{\text{SDW}}$ . Finally, we set  $\xi_{\text{SDW}} = 5a$  throughout our calculations, varying the correlation length of the Néel fluctuations  $\xi_{\text{Néel}}$ . Our results do not change significantly for smaller values of  $\xi_{\text{SDW}}$ .

To obtain the transition temperatures in the  $s$  and  $d$ -wave channels, we linearize the Eliashberg equations in the superconducting quantities and solve the resulting equations for the anomalous component  $W_{\alpha,n}$  and the normal component  $Z_{\alpha,n} = \text{Im} \Sigma_{\alpha,n}^N / i\omega_n$  of the self-energy (the real part of  $\Sigma^N$  just renormalizes the band dispersions, possibly differently for different pockets [16,17,31]). These quantities are averaged over each Fermi pocket, becoming functions only of the Fermi pocket label  $\alpha$  and the fermionic Matsubara frequency  $\omega_n = (2n + 1)\pi T$ . With the aid of the auxiliary “gap functions”

$\bar{\Delta}_{\Gamma,n} \equiv W_{\Gamma,n}/(Z_{\Gamma,n}|\omega_n|\sqrt{N_X})$  and  $\bar{\Delta}_{(X/Y),n} \equiv W_{(X/Y),n}/(Z_{X,n}|\omega_n|\sqrt{N_\Gamma})$ , the linearized gap equation is expressed as a matrix equation in Matsubara (indices  $n, m$ ) and band (indices  $\alpha, \beta$ ) spaces  $\sum_{m,\beta} K_{nm}^{\alpha\beta} \bar{\Delta}_{\beta,m} = 0$ , with the kernel

$$(K_{nm}^{\alpha\beta}) = - \begin{pmatrix} \delta_{nm} \frac{Z_{\Gamma,n}|\omega_n|}{T} & \frac{\lambda_{\text{SDW}}}{2} a_{nm}^{(1)} & \frac{\lambda_{\text{SDW}}}{2} a_{nm}^{(1)} \\ \lambda_{\text{SDW}} a_{nm}^{(1)} & \delta_{nm} \frac{Z_{X,n}|\omega_n|}{T} & \lambda_{\text{Neel}} a_{nm}^{(2)} \\ \lambda_{\text{SDW}} a_{nm}^{(1)} & \lambda_{\text{Neel}} a_{nm}^{(2)} & \delta_{nm} \frac{Z_{X,n}|\omega_n|}{T} \end{pmatrix} - \frac{1}{2} \left[ \frac{\mu^*}{1+r} - \frac{\tau^{-1}}{T} \frac{\delta_{nm}}{r} \right] \begin{pmatrix} 2 & \sqrt{r} & \sqrt{r} \\ 2\sqrt{r} & r & r \\ 2\sqrt{r} & r & r \end{pmatrix}. \quad (2)$$

Here, we have introduced the matrix elements coming from the bosonic modes  $a_{nm}^{(i)} = a^i(\omega_n - \omega_m)$  ( $i = 1$  corresponds to SDW and  $i = 2$  to Néel fluctuations) and the dimensionless coupling constants  $\lambda_{\text{SDW}} = 2g_{\text{SDW}}^2\sqrt{N_\Gamma N_X}$ ,  $\lambda_{\text{Neel}} = g_{\text{Neel}}^2 N_X$ ;  $T$  is the temperature. We also introduce an upper frequency cutoff  $\Lambda = 8\gamma_{\text{SDW}}$ , corresponding to the energy scale of the bottom (top) of the electron (hole) bands, and we assume that  $\mu^*$  is a bare Coulomb interaction renormalized in the standard way by higher energy processes. The scattering rate associated with nonmagnetic point impurities is represented by  $\tau^{-1}$ , and the  $Z_{\alpha,n}$  functions are obtained analytically (see Supplemental Material [30]). The Coulomb pseudopotential favors solutions with  $\sum_{\alpha} N_{\alpha} \Delta_{\alpha} = 0$ .

Reflecting the tetragonal symmetry of the system, the matrix equation supports two different types of solution: the  $s$ -wave state  $\bar{\Delta}_{X,n} = \bar{\Delta}_{Y,n}$ , with either  $s^{++}$  ( $\bar{\Delta}_{\Gamma,n} \propto \bar{\Delta}_{X,n}$ ) or  $s^{+-}$  ( $\bar{\Delta}_{\Gamma,n} \propto -\bar{\Delta}_{X,n}$ ) structure, and the  $d$ -wave state  $\bar{\Delta}_{X,n} = -\bar{\Delta}_{Y,n}$ . The solution in a given symmetry channel is obtained when the largest eigenvalue  $\eta$  of the matrix (2) vanishes. Since our calculations never yield an  $s^{++}$  state, we use the terms  $s$ -wave and  $s^{+-}$  to refer to the same state. Because of limitations of the size of the matrices that can be diagonalized and since the matrix size scales as  $\Lambda/T$ , we resolve  $T_c \geq 10^{-3} \gamma_{\text{SDW}}$ . Hereafter, we set  $\lambda_{\text{SDW}} = 0.4$  and the Coulomb pseudopotential  $\mu^* = 0.8$ , which gives, in the absence of competing Néel fluctuations,  $T_{c,0}^{s\text{-wave}} \approx 30$  K and implies  $\lambda_{\text{Neel}} = 0.8$ .

Figure 2 shows our principal results: the dependence of the SC transition temperature  $T_c$  on the strength of Néel fluctuations (parametrized by the Néel correlation length  $\xi_{\text{Neel}}$ ). The light solid line (red online) shows the transition temperature  $T_c^{s\text{-wave}}$  for the  $s^{+-}$  channel in the absence of impurity scattering. Surprisingly, even weak short-range fluctuations strongly suppress  $s^{+-}$  SC, but once  $T_c^{s\text{-wave}}$  has been substantially reduced, the additional suppression effect caused by further increasing  $\xi_{\text{Neel}}$  is small. Sufficiently strong Néel correlations produce a  $d$ -wave solution (heavier solid line, blue online) with  $T_c^{d\text{-wave}}$  that eventually becomes larger than  $T_c^{s\text{-wave}}$  but always remains small compared to the maximum  $T_c^{s\text{-wave}}$ . In our linearized theory, the transition between  $s$ -wave and

$d$ -wave superconductors appears as a discontinuous change in the nature of the state, but the considerations of Ref. [23] suggest that nonlinear terms not included here will generate an intermediate  $s + id$  state (shaded area). The dashed lines show the behavior in the presence of impurity scattering, which is pair breaking for both  $s^{+-}$  and  $d$ -wave superconductivity. Sufficiently strong impurity scattering can disconnect the two SC states, leaving an intermediate non-SC regime.

We also analyze the impact of the Coulomb pseudopotential  $\mu^*$  on the  $s^{+-}$  state—the  $d$ -wave state avoids the Coulomb repulsion. Figure 3 shows the pocket-averaged  $s^{+-}$  gap function  $\sum_{\alpha} N_{\alpha} \Delta_{\alpha}$  both in the presence and in the absence of  $\mu^*$ . To avoid the local repulsion, the averaged order parameter changes sign at a nonzero Matsubara frequency, although the sign of each individual gap does not necessarily change. This is the multiband analogue of the response of a single-band  $s$ -wave superconductor to the local repulsion. For all values of  $\xi_{\text{Neel}}$  we have studied, neither  $\Delta_{n=0}$  nor  $T_c^{s\text{-wave}}$  (shown in the inset) are substantially altered by  $\mu^*$ , in agreement with the weak-coupling analysis of Ref. [32].

We now turn to the physics of the decrease of  $T_c^{s\text{-wave}}$  caused by Néel fluctuations. Increasing  $\xi_{\text{Neel}}$  increases the spin fluctuation intensity and changes its functional form (see the inset of Fig. 2). To analyze how different frequency regions of the Néel spectral function affect  $T_c^{s\text{-wave}}$ , we follow Refs. [25,26] and calculate the functional derivative

$$\frac{1}{T_c} \frac{\omega \delta T_c}{\delta A_{\text{Neel}}(\omega)} = \left[ \hat{\Delta} \frac{\omega \delta \hat{K}}{T_c \delta A_{\text{Neel}}(\omega)} \hat{\Delta} \right] / \left( -\frac{\partial \eta}{\partial T_c} \right)_{\eta=0} \quad (3)$$

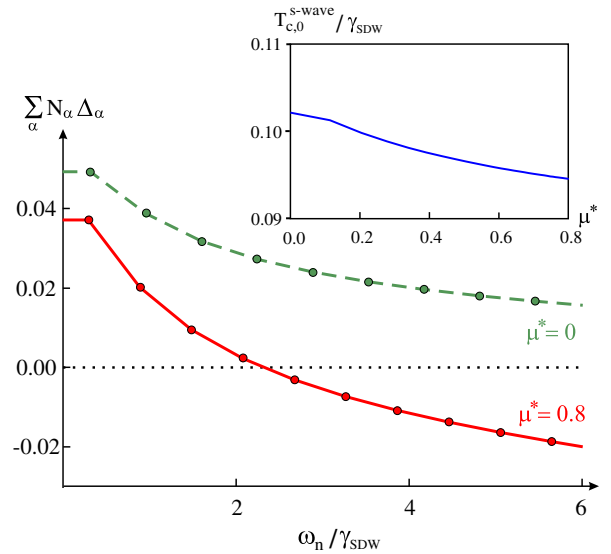


FIG. 3 (color online). Averaged  $s^{+-}$  gap function  $\sum_{\alpha} N_{\alpha} \Delta_{\alpha}$  across the different pockets at  $T_{c,0}^{s\text{-wave}}$  as a function of Matsubara frequency  $\omega_n$  (in units of  $\gamma_{\text{SDW}}$ ), for  $\mu^* = 0$  (green dashed curve) and  $\mu^* = 0.8$  (red solid curve). The inset shows  $T_{c,0}^{s\text{-wave}}$  (in units of  $\gamma_{\text{SDW}}$ ) as a function of  $\mu^*$ . Although here we used  $\xi_{\text{Neel}} = 0$ , a similar behavior holds for  $\xi_{\text{Neel}} \neq 0$ .

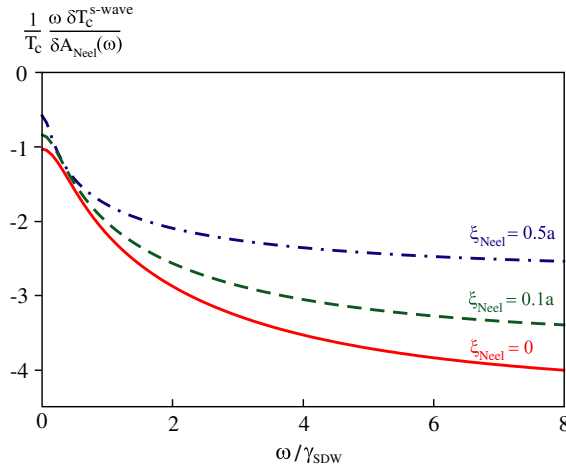


FIG. 4 (color online). Functional derivative  $T_c^{-1} \omega \delta T_c^{s\text{-wave}} / \delta A_{\text{Neel}}(\omega)$  as a function of frequency  $\omega$  (in units of  $\gamma_{\text{SDW}}$ ) for the cases  $\xi_{\text{Neel}} = 0$  (red solid line),  $\xi_{\text{Neel}} = 0.1a$  (green dashed line), and  $\xi_{\text{Neel}} = 0.5a$  (blue dot-dashed line).

for different values of  $\xi_{\text{Neel}}$ , as shown in Fig. 4. Previous work [25,26] has shown that the low-frequency regime captures the pair-breaking effects of inelastic scattering while the high frequency regime expresses the changes to the pairing interaction. The larger magnitude of  $\delta \log T_c / \delta A_{\text{Neel}}$  at high frequencies shows that in the pnictides the dominant effect of the Néel fluctuations is to provide a negative contribution to the  $s^{+-}$  pairing interaction, with the extra pair-breaking effect of the induced low-frequency inelastic scattering being less important. Because Fig. 4 shows that the logarithmic derivative of  $T_c$  is a slow function of  $\xi_{\text{Neel}}$ , we conclude that the initial steep drop and subsequent flattening of the  $T_c$  curve shown in Fig. 2 is due in large part to the variation of  $T_c$  itself. Additionally, as  $\xi_{\text{Neel}}$  is increased the Néel fluctuation spectrum shifts to lower frequencies (see the inset of Fig. 2), where the pair-breaking is less effective. However, additional physics is also at play. In the weak-coupling limit of two effective competing pairing interactions  $\lambda_s$  and  $\lambda_d$ , we obtain  $T_c \propto \exp[-1/(\sqrt{\lambda_s^2 + \lambda_d^2} - \lambda_d)]$  so

$$\frac{d \log T_c}{d \lambda_d} \propto - \frac{1}{(\lambda_s^2 + \lambda_d^2 - \lambda_d \sqrt{\lambda_s^2 + \lambda_d^2})}, \quad (4)$$

which is larger in magnitude for larger  $\lambda_d$ , implying an opposite ordering of the curves to that seen in Fig. 4. Our Eliashberg results and Eq. (4) differ because the gap function self-consistently adjusts to the pairing potential, so that for larger  $\xi_{\text{Neel}}$  values the gap function decreases more rapidly with frequency, thereby minimizing the depairing effects of the Néel fluctuations (see Supplemental Material [30]).

Our results offer a possible explanation for the puzzling behavior of the hole-doped  $\text{Ba}(\text{Fe}_{1-x}\text{M}_x)_2\text{As}_2$  series ( $M = \text{Mn, Cr, Mo}$ ) [10], which in contrast to its electron-doped counterpart ( $M = \text{Co, Ni, Rh, Pt, Cu}$ ) [12] does not display

SC. The short-range Néel fluctuations induced by the dopants, which were observed experimentally for low concentrations of  $M = \text{Mn}$  [8,9], suppress the  $s^{+-}$  state without giving rise to a high-temperature  $d$ -wave state. This low- $T_c$   $s^{+-}$  state, in turn, can be easily suppressed, for example, by impurity scattering or by another competing ordered state, such as the SDW state [33,34] observed at low  $x$ . We suggest that improving the purity of the samples and applying pressure to suppress the SDW state may reveal either a weakened  $s^{+-}$  state or perhaps a low  $T_c$   $d$ -wave state. Similarly, in the extremely electron-doped  $\text{A}_y\text{Fe}_{2-x}\text{Se}_2$  systems [13,35,36], where for small  $y$  the hole pocket is generally absent and  $d$ -wave superconductivity is discussed, adding holes by changing  $A$  [14] or by applying pressure [15] should produce the reverse competition. Interestingly, recent pressure experiments found two separate SC domes in  $\text{K}_{0.8}\text{Fe}_{1.78}\text{Se}_2$  [37], which could be related to the behavior shown in Fig. 2 (dashed lines). Indeed, pressure changes the shapes of the Fermi pockets, which affects the relative strength of SDW and Néel fluctuations.

More generally, since most FeSC compounds have two matching electron pockets separated by  $\mathbf{Q}_{\text{Neel}}$  even at optimal doping compositions, we expect at least weak Néel-type fluctuations. Indeed, recent Raman data indicate that a  $d$ -wave instability, presumably originated from these Néel fluctuations, competes with the  $s^{+-}$  state of optimally doped FeSC [38]. However, our findings show that these weak  $(\pi, \pi)$  fluctuations strongly suppress  $T_c^{s\text{-wave}}$ . This suggests that the highest  $T_c$  in several FeSCs can be potentially enhanced if the  $(\pi, \pi)$  fluctuations are minimized. One possible route is to make the sizes and shapes of the two electron pockets unequal, via, for example, a tetragonal symmetry breaking [39]. Interestingly, torque magnetometry measurements found such a tetragonal symmetry breaking above  $T_c$  in some optimally doped FeSCs [40]. In Ref. [41], it was also observed that a small strain applied along the orthorhombic axis can enhance  $T_c$ .

In summary, our results open a new route to explore unconventional superconductivity in multiband systems by controlling competing spin fluctuations. In particular, Néel fluctuations have a strong effect on the  $s^{+-}$  state of the FeSCs, rapidly reducing  $T_c$  and potentially driving a transition from  $s$ -wave to  $d$ -wave SC (Fig. 2). Depending on the strength of impurity scattering, more exotic states can emerge, such as the  $s + id$  state [23], although this might also arise from other mechanisms [24]. Notice also that the lower  $T_c$  solution, even if not present in the ground state, will give rise to a collective excitation that can in principle be detected by Raman scattering [38,42].

We thank P. Canfield, A. Chubukov, A. Goldman, I. Eremin, A. Kreyssig, B. Lau, R. McQueeney, D. Pratt, J. Schmalian, and G. Tucker for useful discussions. R.M.F. is supported by the NSF Partnerships for International Research and Education (PIRE) Program No. OISE-0968226, and A.J.M. is supported by Grant No. NSF-DMR-1006282.

- \*Present address: School of Physics and Astronomy, University of Minnesota, Minneapolis, MN 55455, USA. rfernand@umn.edu
- [1] K. Ishida, Y. Nakai, and H. Hosono, *J. Phys. Soc. Jpn.* **78**, 062001 (2009); D. C. Johnston, *Adv. Phys.* **59**, 803 (2010); J. Paglione and R. L. Greene, *Nat. Phys.* **6**, 645 (2010); P. C. Canfield and S. L. Bud'ko, *Annu. Rev. Condens. Matter Phys.* **1**, 27 (2010); H. H. Wen and S. Li, *Annu. Rev. Condens. Matter Phys.* **2**, 121 (2011).
  - [2] I. I. Mazin, D. J. Singh, M. D. Johannes, and M. H. Du, *Phys. Rev. Lett.* **101**, 057003 (2008); A. V. Chubukov, D. V. Efremov, and I. Eremin, *Phys. Rev. B* **78**, 134512 (2008); K. Kuroki, S. Onari, R. Arita, H. Usui, Y. Tanaka, H. Kontani, and H. Aoki, *Phys. Rev. Lett.* **101**, 087004 (2008); V. Cvetković and Z. Tesanović, *Phys. Rev. B* **80**, 024512 (2009); J. Zhang, R. Sknepnek, R. M. Fernandes, and J. Schmalian, *Phys. Rev. B* **79**, 220502(R) (2009); A. F. Kemper, T. A. Maier, S. Graser, H-P. Cheng, P. J. Hirschfeld, and D. J. Scalapino, *New J. Phys.* **12**, 073030 (2010).
  - [3] P. J. Hirschfeld, M. M. Korshunov, and I. I. Mazin, *Rep. Prog. Phys.* **74**, 124508 (2011); A. V. Chubukov, *Annu. Rev. Condens. Matter Phys.* **3**, 57 (2012).
  - [4] K. Kuroki, H. Usui, S. Onari, R. Arita, and H. Aoki, *Phys. Rev. B* **79**, 224511 (2009).
  - [5] M. D. Johannes and I. I. Mazin, *Phys. Rev. B* **79**, 220510(R) (2009).
  - [6] M. J. Calderon, G. Leon, B. Valenzuela, and E. Bascones, *Phys. Rev. B* **86**, 104514 (2012).
  - [7] S. Graser, A. F. Kemper, T. A. Maier, H-P. Cheng, P. J. Hirschfeld, and D. J. Scalapino, *Phys. Rev. B* **81**, 214503 (2010).
  - [8] G. S. Tucker, D. K. Pratt, M. G. Kim, S. Ran, A. Thaler, G. E. Granroth, K. Marty, W. Tian, J. L. Zarestky, M. D. Lumsden, S. L. Bud'ko, P. C. Canfield, A. Kreyssig, A. I. Goldman, and R. J. McQueeney, *Phys. Rev. B* **86**, 020503(R) (2012).
  - [9] Y. Texier, Y. Laplace, P. Mendels, J. T. Park, G. Friemel, D. L. Sun, D. S. Inosov, C. T. Lin, and J. Bobroff, *Europhys. Lett.* **99**, 17002 (2012).
  - [10] A. S. Sefat, D. J. Singh, L. H. VanBebber, Y. Mozharivskiy, M. A. McGuire, R. Jin, B. C. Sales, V. Keppens, and D. Mandrus, *Phys. Rev. B* **79**, 224524 (2009); J. S. Kim, S. Khim, H. J. Kim, M. J. Eom, J. M. Law, R. K. Kremer, J. H. Shim, and K. H. Kim, *Phys. Rev. B* **82**, 024510 (2010); M. G. Kim, A. Kreyssig, A. Thaler, D. K. Pratt, W. Tian, J. L. Zarestky, M. A. Green, S. L. Bud'ko, P. C. Canfield, R. J. McQueeney, and A. I. Goldman, *Phys. Rev. B* **82**, 220503(R) (2010); K. Marty, A. D. Christianson, C. H. Wang, M. Matsuda, H. Cao, L. H. VanBebber, J. L. Zarestky, D. J. Singh, A. S. Sefat, and M. D. Lumsden, *Phys. Rev. B* **83**, 060509(R) (2011); A. Pandey, V. K. Anand, and D. C. Johnston, *Phys. Rev. B* **84**, 014405 (2011); A. S. Sefat, K. Marty, A. D. Christianson, B. Saparov, M. A. McGuire, M. D. Lumsden, W. Tian, and B. C. Sales, *Phys. Rev. B* **85**, 024503 (2012); A. Pandey, R. S. Dhaka, J. Lamsal, Y. Lee, V. K. Anand, A. Kreyssig, T. W. Heitmann, R. J. McQueeney, A. I. Goldman, B. N. Harmon, A. Kaminski, and D. C. Johnston, *Phys. Rev. Lett.* **108**, 087005 (2012).
  - [11] A. Thaler, H. Hodovanets, M. S. Torikachvili, S. Ran, A. Kracher, W. Straszheim, J. Q. Yan, E. Mun, and P. C. Canfield, *Phys. Rev. B* **84**, 144528 (2011).
  - [12] P. C. Canfield, S. L. Bud'ko, Ni Ni, J. Q. Yan, and A. Kracher, *Phys. Rev. B* **80**, 060501(R) (2009); N. Ni, A. Thaler, A. Kracher, J. Q. Yan, S. L. Bud'ko, and P. C. Canfield, *Phys. Rev. B* **80**, 024511 (2009); N. Ni, A. Thaler, J. Q. Yan, A. Kracher, E. Colombier, S. L. Bud'ko, P. C. Canfield, and S. T. Hannahs, *Phys. Rev. B* **82**, 024519 (2010).
  - [13] J. Guo, S. Jin, G. Wang, S. Wang, K. Zhu, T. Zhou, M. He, and X. Chen, *Phys. Rev. B* **82**, 180520(R) (2010).
  - [14] T. A. Maier, S. Graser, P. J. Hirschfeld, and D. J. Scalapino, *Phys. Rev. B* **83**, 100515(R) (2011); T. A. Maier, P. J. Hirschfeld, and D. J. Scalapino, *Phys. Rev. B* **86**, 094514 (2012).
  - [15] T. Das and A. V. Balatsky, [arXiv:1208.2468](https://arxiv.org/abs/1208.2468).
  - [16] G. M. Eliashberg, *Sov. Phys. JETP* **11**, 696 (1960).
  - [17] See J. P. Carbotte, *Rev. Mod. Phys.* **62**, 1027 (1990), and references therein.
  - [18] P. Monthoux and D. Pines, *Phys. Rev. Lett.* **69**, 961 (1992).
  - [19] A. J. Millis, *Phys. Rev. B* **45**, 13047 (1992).
  - [20] Ar. Abanov, A. V. Chubukov, and A. M. Finkel'stein, *Europhys. Lett.* **54**, 488 (2001); Ar. Abanov, A. V. Chubukov, and J. Schmalian, *Europhys. Lett.* **55**, 369 (2001); *Adv. Phys.* **52**, 119 (2003); A. V. Chubukov and J. Schmalian, *Phys. Rev. B* **72**, 174520 (2005).
  - [21] R. Roussev and A. J. Millis, *Phys. Rev. B* **63**, 140504(R) (2001).
  - [22] O. V. Dolgov, I. I. Mazin, D. Parker, and A. A. Golubov, *Phys. Rev. B* **79**, 060502(R) (2009); L. Benfatto, E. Cappelluti, and C. Castellani, *Phys. Rev. B* **80**, 214522 (2009); G. A. Ummarino, M. Tortello, D. Daghero, and R. S. Gonnelli, *Phys. Rev. B* **80**, 172503 (2009).
  - [23] V. Stanev and Z. Tesanović, *Phys. Rev. B* **81**, 134522 (2010).
  - [24] R. Thomale, C. Platt, W. Hanke, J. Hu, and B. A. Bernevig, *Phys. Rev. Lett.* **107**, 117001 (2011); C. Platt, R. Thomale, C. Honerkamp, S.-C. Zhang, and W. Hanke, *Phys. Rev. B* **85**, 180502(R) (2012); M. Khodas and A. V. Chubukov, *Phys. Rev. Lett.* **108**, 247003 (2012).
  - [25] A. J. Millis, S. Sachdev, and C. M. Varma, *Phys. Rev. B* **37**, 4975 (1988).
  - [26] D. J. Bergmann and D. Rainer, *Z. Phys.* **263**, 59 (1973).
  - [27] S. Maiti, M. M. Korshunov, T. A. Maier, P. J. Hirschfeld, and A. V. Chubukov, *Phys. Rev. B* **84**, 224505 (2011); *Phys. Rev. Lett.* **107**, 147002 (2011).
  - [28] Y. Wang, J. S. Kim, G. R. Stewart, P. J. Hirschfeld, S. Graser, S. Kasahara, T. Terashima, Y. Matsuda, T. Shibauchi, and I. Vekhter, *Phys. Rev. B* **84**, 184524 (2011).
  - [29] D. S. Inosov, J. T. Park, P. Bourges, D. L. Sun, Y. Sidis, A. Schneidewind, K. Hradil, D. Haug, C. T. Lin, B. Keimer, and V. Hinkov, *Nat. Phys.* **6**, 178 (2010); H.-F. Li, C. Broholm, D. Vaknin, R. M. Fernandes, D. L. Abernathy, M. B. Stone, D. K. Pratt, W. Tian, Y. Qiu, N. Ni, S. O. Diallo, J. L. Zarestky, S. L. Bud'ko, P. C. Canfield, and R. J. McQueeney, *Phys. Rev. B* **82**, 140503(R) (2010).
  - [30] See the Supplemental Material at <http://link.aps.org/supplemental/10.1103/PhysRevLett.110.117004> for details on the solution of the multiband Eliashberg equations.

- [31] L. Benfatto and E. Cappelluti, *Phys. Rev. B* **83**, 104516 (2011).
- [32] I. I. Mazin and J. Schmalian, *Physica (Amsterdam)* **469C**, 614 (2009).
- [33] R. M. Fernandes, D. K. Pratt, W. Tian, J. Zarestky, A. Kreyssig, S. Nandi, M. G. Kim, A. Thaler, N. Ni, P. C. Canfield, R. J. McQueeney, J. Schmalian, and A. I. Goldman, *Phys. Rev. B* **81**, 140501(R) (2010); R. M. Fernandes and J. Schmalian, *Phys. Rev. B* **82**, 014521 (2010).
- [34] A. B. Vorontsov, M. G. Vavilov, and A. V. Chubukov, *Phys. Rev. B* **79**, 060508(R) (2009).
- [35] M. Xu, Q. Q. Ge, R. Peng, Z. R. Ye, Juan Jiang, F. Chen, X. P. Shen, B. P. Xie, Y. Zhang, A. F. Wang, X. F. Wang, X. H. Chen, and D. L. Feng, *Phys. Rev. B* **85**, 220504(R) (2012).
- [36] J. T. Park, G. Friemel, Yuan Li, J.-H. Kim, V. Tsurkan, J. Deisenhofer, H.-A. Krug von Nidda, A. Loidl, A. Ivanov, B. Keimer, and D. S. Inosov, *Phys. Rev. Lett.* **107**, 177005 (2011); G. Friemel, J. T. Park, T. A. Maier, V. Tsurkan, Yuan Li, J. Deisenhofer, H.-A. Krug von Nidda, A. Loidl, A. Ivanov, B. Keimer, and D. S. Inosov, *Phys. Rev. B* **85**, 140511(R) (2012).
- [37] L. Sun *et al.*, *Nature (London)* **483**, 67 (2012).
- [38] F. Kretzschmar *et al.*, [arXiv:1208.5006](https://arxiv.org/abs/1208.5006).
- [39] R. M. Fernandes, A. V. Chubukov, J. Knolle, I. Eremin, and J. Schmalian, *Phys. Rev. B* **85**, 024534 (2012).
- [40] S. Kasahara, H. J. Shi, K. Hashimoto, S. Tonegawa, Y. Mizukami, T. Shibauchi, K. Sugimoto, T. Fukuda, T. Terashima, A. H. Nevidomskyy, and Y. Matsuda, *Nature (London)* **486**, 382 (2012).
- [41] H.-H. Kuo, J. G. Analytis, J.-H. Chu, R. M. Fernandes, J. Schmalian, and I. R. Fisher, *Phys. Rev. B* **86**, 134507 (2012).
- [42] A. Bardasis and J. R. Schrieffer, *Phys. Rev.* **121**, 1050 (1961); D. J. Scalapino and T. P. Devereaux, *Phys. Rev. B* **80**, 140512(R) (2009).